

Searching for dilepton resonances below the Z mass at the LHC

Isaac Hoenig, Gabriel Samach, and David Tucker-Smith

Department of Physics, Williams College, Williamstown, MA 01267

(Dated: October 14, 2014)

Abstract

We consider LHC searches for dilepton resonances in an intermediate mass range, $\sim 10 - 80$ GeV. We adopt a kinetically mixed Z' as an example of weakly coupled new physics that might have evaded detection at previous experiments but which could still be probed by LHC dilepton spectrum measurements in this mass range. Based on Monte Carlo simulations, we estimate that existing data from the 7 and 8 TeV LHC could be used to test values of the kinetic mixing parameter ϵ several times smaller than precision electroweak upper bounds, were an appropriate analysis to be carried out by one of the experimental collaborations.

I. INTRODUCTION

The appearance of a new dilepton resonance at the Large Hadron Collider (LHC) would mean the discovery of physics beyond the Standard Model (SM). Both ATLAS and CMS have searched for dilepton resonances, focusing mainly on the high-mass region above ~ 100 GeV. Here we argue that there is something to be gained by searching at lower masses – we focus on the $\sim 10 - 80$ GeV mass range, above the masses of the heaviest hadronic bound states and below the Z peak. To explore whether LHC searches in this mass range could probe parameter space not already excluded by previous experiments we adopt a particular model for a weakly coupled dilepton resonance: a kinetically mixed Z' [1]. A kinetically mixed Z' is a simple addition to the SM. It is also a central feature in certain models of dark matter [2–10].

For our purposes, the kinetically mixed Z' scenario is parameterized by the Z' mass $M_{Z'}$ and the kinetic mixing parameter ϵ , which controls the coupling strength of the Z' to SM particles. We use Monte Carlo simulations to estimate the potential sensitivity of specialized analyses of existing 7 and 8 TeV data to a kinetically mixed Z' , and to estimate the potential sensitivity of 14 TeV data in the longer term. We also investigate whether the CMS analysis of the dilepton invariant-mass spectrum at 7 TeV [11] implies interesting upper bounds on ϵ for various intermediate $M_{Z'}$ values, although this exercise is no substitute for an analysis carried out by an experimental collaboration.

Our main results are summarized in Figure 9. We find that CMS results presented in Ref. [11] imply upper bounds on ϵ that lie below precision electroweak upper bounds in the 30 – 70 GeV mass range. More specialized analyses of existing data could probe ϵ values as small as a factor of ~ 5 below precision electroweak upper bounds. The analyses we test start with standard muon p_T cuts used in CMS analyses (14 and 9 GeV for the dimuon pair for $\sqrt{s} = 7$ TeV, and 20 and 10 GeV for $\sqrt{s} = 8$ TeV), but would still be sensitive to $\epsilon \lesssim 10^{-2}$ for Z' masses as small as $M_{Z'} \sim 12$ GeV, although for $M_{Z'}$ below 14 GeV the CMS search for a light pseudoscalar decaying to $\mu^+\mu^-$ already implies exclusion down to significantly smaller values of ϵ [12].

We focus on a kinetically mixed Z' , but can conclude more generally that, even for dilepton resonances below M_Z , the LHC can compete with previous experimental probes. Our results suggest that it would be worthwhile for LHC experimental collaborations to carry

out analyses searching for dilepton resonances in the intermediate mass range considered here. One can interpret our sensitivity estimates in the context of a different model by using the cross sections of Table I and the fact that the production cross section is proportional to ϵ^2 , to convert the ϵ values of Figure 9 to $\sigma(pp \rightarrow Z' \rightarrow l^+l^-)$ values.

In the following section we review the kinetically mixed Z' model and current experimental constraints. In Section III we describe our simulation and analysis methods and present sensitivity estimates for 7 TeV data. In Section IV we present sensitivity estimates for 8 TeV data and, under certain assumptions, for the 14 TeV LHC.

II. A KINETICALLY MIXED Z'

The model we consider is defined by the Lagrangian

$$\mathcal{L} = \mathcal{L}_{SM} - \frac{1}{4}B'_{\mu\nu}B'^{\mu\nu} - \frac{\epsilon}{2}B_{\mu\nu}B'^{\mu\nu} + \frac{M_{B'}^2}{2}B'_\mu B'^\mu + \dots, \quad (1)$$

where \mathcal{L}_{SM} is the SM Lagrangian, $B_{\mu\nu}$ is the hypercharge field strength tensor, and $B'_{\mu\nu}$ is the field strength tensor for a new $U(1)'$ gauge field. The mass for the $U(1)'$ gauge field, $M_{B'}$, can be generated by the vacuum expectation value of a SM-singlet scalar field Φ charged under the $U(1)'$, whose Lagrangian terms we do not write explicitly. The phenomenology of Φ can be interesting in its own right, but we do not consider it here. The collider implications of $U(1)'$ gauge bosons in this type of setup have previously been considered in Refs. [10, 13–31], for example.

The neutral $SU(2)$, $U(1)$ and $U(1)'$ gauge fields W_μ^3 , B_μ , and B'_μ are related to mass-eigenstate gauge fields with diagonal and canonically normalized kinetic terms, A_μ , Z_μ , and Z'_μ , by

$$\begin{pmatrix} B_\mu \\ W_\mu^3 \\ B'_\mu \end{pmatrix} = \begin{pmatrix} c_w & -\left(s_w c_z + \frac{\epsilon}{\sqrt{1-\epsilon^2}} s_z\right) & \left(s_w s_z - \frac{\epsilon}{\sqrt{1-\epsilon^2}} c_z\right) \\ s_w & c_w c_z & -c_w s_z \\ 0 & \frac{1}{\sqrt{1-\epsilon^2}} s_z & \frac{1}{\sqrt{1-\epsilon^2}} c_z \end{pmatrix} \begin{pmatrix} A_\mu \\ Z_\mu \\ Z'_\mu \end{pmatrix}, \quad (2)$$

where c_w and s_w are cosine and sine of the weak mixing angle, and c_z and s_z are cosine and sine of the angle that parameterizes $Z - Z'$ mixing, determined by

$$\tan 2\theta_z = \frac{2\epsilon\sqrt{1-\epsilon^2} s_w \overline{M}_Z^2}{\overline{M}_Z^2(1-\epsilon^2-s_w^2\epsilon^2) - M_{B'}^2}. \quad (3)$$

Here \overline{M}_Z is the SM value for the mass of the Z boson, *i.e.* its value in the $\epsilon \rightarrow 0$ limit.

One can use the field transformation of Equation (2) and the charges of SM fermions under the SM gauge group to calculate the couplings of SM fermions to the Z' . If both

$$\epsilon \ll 1 \quad \text{and} \quad \left| \frac{\epsilon s_w \bar{M}_Z^2}{\bar{M}_Z^2 - M_{B'}^2} \right| \ll 1 \quad (4)$$

are satisfied, we can work to first order in ϵ , giving

$$\theta_z \simeq \frac{\epsilon s_w \bar{M}_Z^2}{\bar{M}_Z^2 - M_{B'}^2}. \quad (5)$$

In this regime, the couplings of the Z' to SM fermions are

$$g_{\bar{f}fZ'} \simeq -\epsilon \left(\frac{\bar{M}_Z^2 c_w e Q_f - M_{B'}^2 g_y Y_f}{\bar{M}_Z^2 - M_{B'}^2} \right), \quad (6)$$

where e and g_y are the electromagnetic and hypercharge gauge couplings, Q_f and Y_f are the electric charge and hypercharge of the fermion, and where we use the notation

$$\mathcal{L} \supset \sum_f g_{\bar{f}fZ'} \bar{f} \gamma^\mu f Z'_\mu, \quad (7)$$

with $f = e_L, e_R$, and so on. When either $M_{B'} \ll \bar{M}_Z$ or $M_{B'} \gg \bar{M}_Z$ is satisfied we can further approximate Equation (6) as

$$g_{\bar{f}fZ'} \simeq \begin{cases} -\epsilon c_w e Q_f & M_{B'} \ll \bar{M}_Z \\ -\epsilon g_y Y_f & M_{B'} \gg \bar{M}_Z. \end{cases} \quad (8)$$

In the context of a dark matter model, the Z' might have a sizable branching ratios to dark-sector final states. In this work we assume that the Z' decays exclusively to SM states. This possibility fits in naturally with viable dark matter models, even for small values of ϵ . For example, if the dark matter is a fermion χ charged under $U(1)'$, Z' decays to χ pairs are forbidden for $M_\chi > M_{Z'}/2$, and for $M_\chi > M_{Z'}$ the χ relic abundance can be regulated by the annihilation process $\chi \chi^{(-)} \rightarrow Z' Z'$ for an appropriate value of the $U(1)'$ gauge coupling g' [32]. For the parameter region relevant to the collider studies considered in this paper (M'_Z in the $\sim 10 - 80$ GeV range and $\epsilon > 10^{-3}$) results from LUX [33] rule out this $\chi \chi^{(-)} \rightarrow Z' Z'$ scenario for the case where the dark matter is a Dirac fermion, but the Majorana case is viable. A Majorana mass can be generated by $\Phi - \chi$ interactions for suitably chosen $U(1)'$ charges.

Although dark matter offers one motivation to search for weakly coupled dilepton resonances, our results do not depend on the possible connection to dark matter. The key assumption is that the width of the dilepton resonance is dominated by SM final states.

Experimental and observational constraints on the kinetically mixed Z' scenario are summarized in Ref. [34]. In the $\sim 10\text{--}80$ GeV mass range that interests us, precision electroweak constraints require $\epsilon \lesssim (2-3) \times 10^{-2}$ [25]. If the Z' decays dominantly to SM states, as assumed here, there are also constraints from PEP, PETRA, and TRISTAN measurements of the $e^+e^- \rightarrow \text{hadrons}$ cross sections at various center-of-mass energies. As shown in Ref. [25], these constraints are stronger than those from precision electroweak measurements at particular values of $M_{Z'}$ close to the experiments' center-of-mass energies, but they do not cover the mass range continuously.

At higher masses, LHC searches for high-mass dilepton resonances can be used to constrain the kinetically mixed Z' scenario. These constraints were derived in Ref. [30] using 7 TeV LHC results. Figure 1 shows the upper bounds on ϵ implied by ATLAS [35] and CMS [36] 8 TeV results. To obtain these constraints we calculate the cross section

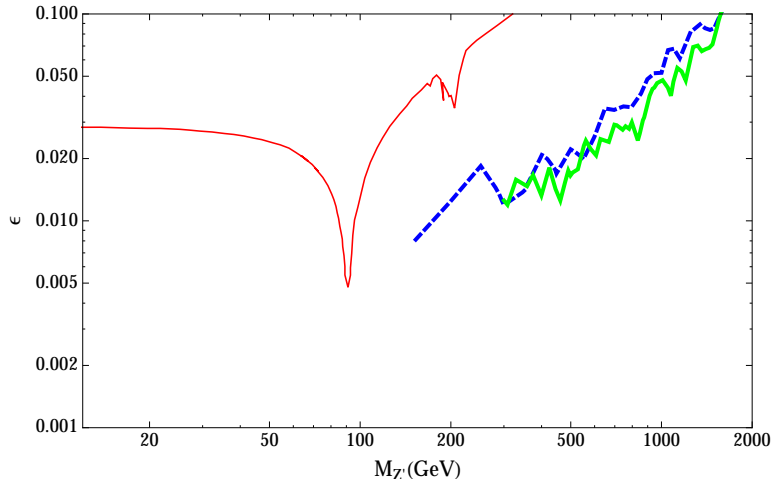


FIG. 1. 95% CL upper bounds on ϵ from ATLAS [35] (dashed blue line) and CMS [36] (thick green line) searches for high-mass dilepton resonances, along with the precision electroweak constraint taken from Ref. [25] (thin red line).

for $pp \rightarrow Z' \rightarrow l^+l^-$ at leading order using Madgraph [37] with CTEQ66 [38, 39] parton distribution functions, and apply a mass-dependent NNLO K-factor determined using the

ZWPROD code [40, 41].

Given how successful LHC searches for high-mass dilepton resonances have been at probing new parameter space for the kinetically mixed Z' scenario, a natural question is whether LHC data can be used to probe new parameter space for $M_{Z'} < M_Z$. The results of a CMS search for a light pseudoscalar Higgs in the dimuon channel, which relied on a specialized trigger, imply a limit on ϵ for $M_{Z'}$ in the 5.5 – 14 GeV mass range [12] (for an earlier ATLAS analysis, see Ref. [42]). For example, assuming equal acceptances for the Z' and the pseudoscalar, we find that the CMS upper limit implies $\epsilon < 2 \times 10^{-3}$ for $M_{Z'} = 12$ GeV. In the following sections we consider whether LHC studies of the dimuon invariant mass distribution could in principle be used to probe the kinetically mixed Z' model for a broader range of intermediate Z' masses. From simulations with standard cuts taken from existing analyses, we find that current data could be used to probe ϵ values well below the precision electroweak limit for much of the mass range below M_Z , although not down to the $\epsilon \sim 2 \times 10^{-3}$ level probed by the CMS pseudoscalar search for masses below 14 GeV. It is possible that Tevatron data could also be used to probe ϵ values below precision electroweak upper bounds. Our rough estimates suggest that it is unlikely that the sensitivity of Tevatron data would exceed that of LHC data, but we have not investigated the Tevatron sensitivity in detail.

III. POTENTIAL SENSITIVITY OF 7 TEV LHC DATA

A. simulation methods

We perform Monte Carlo simulations of dimuon production to estimate the sensitivity of LHC data to the kinetically mixed Z' model for $M_{Z'} < M_Z$. We implement the model in FeynRules [43] and simulate both the Z' signal and the dominant Drell-Yan background using MadGraph5 [37] and Pythia 6.4 [44], with Madgraph's implementation of MLM matching [45] turned on, and up to two jets included at matrix element level. We approximate detector resolution effects by performing a Gaussian smearing of the p_T 's of the muons using the

smearing function

$$\frac{\sigma_{p_T}}{p_T} = \begin{cases} 0.03 & |\eta| < 1.5 \text{ and } p_T < 200 \\ 0.04 & |\eta| \geq 1.5 \text{ and } p_T < 200 \\ 0.05 & p_T \geq 200 \end{cases} \quad (9)$$

This smearing function is consistent with the settings in the default CMS card for the Delphes 3.0 fast detector simulator, which have been shown to give reasonable agreement with data [46]. The sizes of our background Monte Carlo samples correspond to effective luminosities roughly a factor of ten times larger than the luminosities used for the associated analyses.

Drell-Yan production in the mass range that interests us has been studied at 7 TeV by ATLAS [47] and CMS [11]. In this section we will frequently refer to the CMS analysis, which uses an integrated luminosity of 4.5 fb^{-1} . Figure 1 of that paper shows that, for the selection cuts used, Drell Yan production accounts for approximately 90% of dimuon production in the mass range that interests us. The CMS analysis requires the leading and subleading muons to have $(p_T)_1 > 14 \text{ GeV}$ and $(p_T)_2 > 9 \text{ GeV}$, respectively, with both muons' pseudorapidities satisfying $|\eta| < 2.4$. For these cuts, Figure 2 compares the dimuon invariant-mass distribution produced by our simulations with that produced by the CMS full simulation of the Drell-Yan process, as reported in Ref. [11]. We rescale our distribution to produce the same number of events as the CMS simulation in the $60 - 120 \text{ GeV}$ mass range. We find agreement at the 5% level for the bins in the $25 - 76 \text{ GeV}$ mass range. Larger discrepancies approaching 15% are evident in the two lowest-mass bins, where higher order effects are most important. Larger discrepancies are also evident around the Z mass, where the bin counts depend sensitively on the muon momentum resolution. Our simulations give a Z peak that is slightly too short and broad, suggesting that we are not unreasonably optimistic in our estimation of the resolution.

A light kinetically mixed Z' can also be searched for in the dielectron channel, and combining dimuon and dielectron results would likely lead to improved sensitivity. For simplicity we restrict our attention to the dimuon channel, in part because, as shown in Figure 3 of Ref. [11], the efficiency in the dielectric channel is significantly lower in the invariant mass range that interests us.

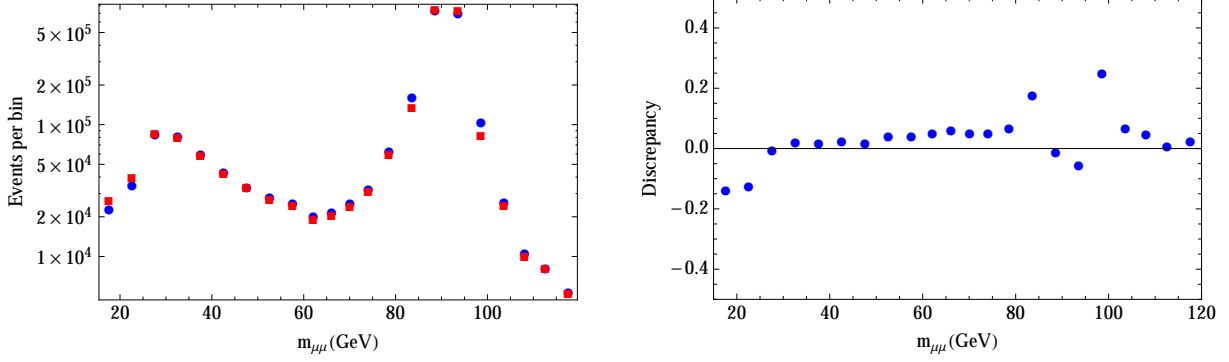


FIG. 2. Left: with $\sqrt{s} = 7$ TeV and an integrated luminosity of 4.5 fb^{-1} , a comparison between the Drell-Yan dimuon invariant-mass distributions predicted by CMS simulations (red squares) and by our simulations (blue circles). The muons are required to have $(p_T)_1 > 14$ GeV, $(p_T)_2 > 9$ GeV, and $|\eta| < 2.4$. We rescale our $m_{\mu\mu}$ distribution to give the same total counts as the CMS simulation in the $60 - 120$ GeV mass range. Right: discrepancies between our simulated bin counts and those of CMS.

B. A benchmark scenario: $M_{Z'} = 50$ GeV, $\epsilon = 0.02$

To establish that a Z' signal would be detectable at the LHC for parameters consistent with precision electroweak bounds, we adopt the parameter point ($M_{Z'} = 50$ GeV, $\epsilon = 0.02$), which lies slightly below the precision electroweak exclusion contour in Figure 1. We normalize our background invariant-mass distribution to data, using the number of events reported in the $60 - 120$ GeV mass range in the CMS analysis of Ref. [11]. To normalize the signal we use the matched cross section calculated by MadGraph with CTEQ66 parton distributions [38, 39] and, in addition to selection cuts, we apply an efficiency of 75%, consistent with or slightly below the efficiencies reported in Ref. [11]. Signal cross sections calculated by MadGraph for various Z' masses are given in Table I.

The invariant mass distribution for signal plus background for $M_{Z'} = 50$ GeV and $\epsilon = 0.02$, using 1 GeV bins, is shown in Figure 3. For the parameters of this benchmark scenario, the Z' signal would be clearly visible in 7 TeV data, motivating us to investigate further the potential sensitivity of the LHC to the kinetically mixed Z' model in the $M_{Z'} < M_Z$ regime.

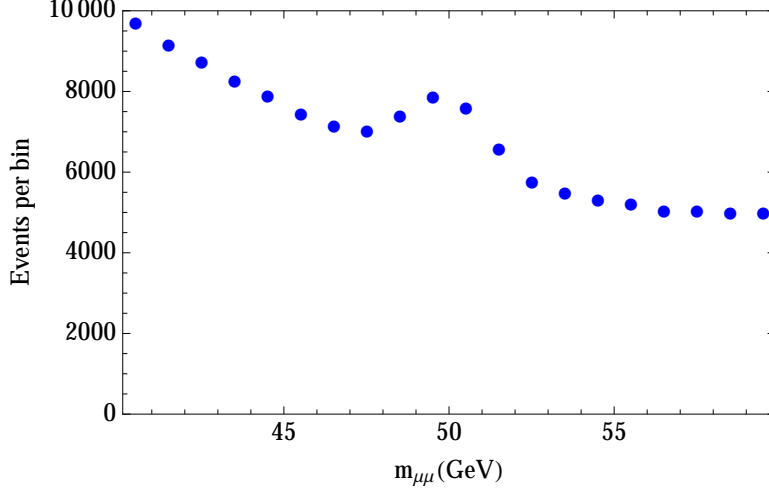


FIG. 3. With $\sqrt{s} = 7$ TeV and an integrated luminosity of 4.5 fb^{-1} , simulated signal plus background for the benchmark parameter point $M_{Z'} = 50$ GeV and $\epsilon = 0.02$. The muons are required to have $(p_T)_1 > 14$ GeV, $(p_T)_2 > 9$ GeV, and $|\eta| < 2.4$. We normalize background to data and apply a 75% efficiency to signal.

C. Models for the dimuon invariant mass distributions

To estimate the ϵ reach of 7 TeV LHC data, we adopt models for the background and signal invariant mass distributions. We model the signal using the invariant mass bin counts produced by our Monte Carlo simulations. Throughout we apply a 75% efficiency to the signal. For the background we employ a more flexible model that allows for deviations of actual SM $m_{\mu\mu}$ distributions from those predicted by simulations. The bin counts predicted by our background model are

$$b_i(\theta, \delta) = p_i(\theta)(1 + \delta_i), \quad (10)$$

where p_i represents a fifth-order polynomial with coefficients θ , and the δ_i are additional nuisance parameters, one for each bin. When we incorporate a possible signal the predicted bin counts become

$$\nu_i(\mu, \theta, \delta) = \mu s_i + b_i(\theta, \delta), \quad (11)$$

where s_i are the Monte-Carlo derived signal bin counts for particular pair of $(\epsilon, M_{Z'})$ values, and μ controls the signal strength.

We quantify the compatibility of signal strength μ with data n_i by

$$\chi^2(\mu) = \min_{\{\theta, \delta\}} \left\{ \sum_i \left[\frac{[n_i - \nu_i(\mu, \theta, \delta)]^2}{\nu_i(\mu, \theta, \delta)} + \left(\frac{\delta_i}{\kappa} \right)^2 \right] \right\}. \quad (12)$$

In this expression, the background parameters θ and δ are set to their best-fit values for signal strength μ . That is, they are chosen to minimize the quantity in brackets. The δ parameters are effectively associated with fake measurements of uncertainty κ . In the $\kappa \rightarrow 0$ limit the background model reduces to a fifth-order polynomial. We describe how we choose κ values below.

Taking the signal strength to zero and neglecting the δ parameters (or equivalently, sending $\kappa \rightarrow 0$), we can identify the θ parameters that give the best fifth-order polynomial fit to our Drell-Yan Monte Carlo $m_{\mu\mu}$ distribution. Figure 4 shows this fit for the 35 – 75 GeV mass range. At lower masses, matters are complicated by the fact that the muon p_T

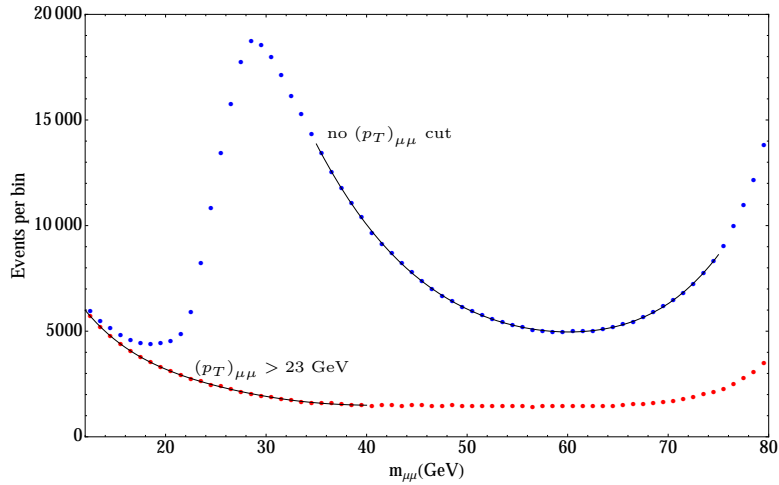


FIG. 4. For $\sqrt{s} = 7$ TeV and an integrated luminosity of 4.5 fb^{-1} , our simulated Drell-Yan $m_{\mu\mu}$ distributions with and without the $(p_T)_{\mu\mu}$ cut, along with best-fit fifth-order polynomial curves. The muons are required to have $(p_T)_1 > 14$ GeV, $(p_T)_2 > 9$ GeV, and $|\eta| < 2.4$.

cuts produce a peak in the invariant mass distribution near $m_{\mu\mu} = 30$ GeV. Dimuon masses below ~ 30 GeV require the dimuon system to recoil off of a jet or jets in order to satisfy $(p_T)_1 > 14$ GeV and $(p_T)_2 > 9$ GeV.

A cut on $(p_T)_{\mu\mu}$, the transverse momentum of the dimuon system, can be used to probe Z' masses below ~ 30 GeV. We choose the cut on $(p_T)_{\mu\mu}$ to be equal to the sum of the two individual muon p_T thresholds, 23 GeV for the muon p_T cuts used in the CMS analysis of

Ref. [11]. With this choice, an event with very small $m_{\mu\mu}$ that passes the individual muon p_T cuts will also pass the cut on $(p_T)_{\mu\mu}$. Here and for all of our analyses we require that the separation between the μ^+ and μ^- satisfies $\Delta R > 0.3$. Figure 4 shows the best fifth-order polynomial fit for the 12 – 40 GeV mass range when this additional cut is applied to our Drell-Yan Monte Carlo sample.

To calculate a p -value for the background-model fit to a given data set n_i , we first use Equation (12) to calculate $\chi^2(0)$ and extract best-fit background parameters $\theta_{(0)}$ and $\delta_{(0)}$. We define the p -value for the fit to be

$$p = \int_{\chi^2(0)}^{\infty} f(x; n_d) dx, \quad (13)$$

where $f(x; n_d)$ is the probability distribution function for the chi squared distribution with n_d degrees of freedom, and we take n_d equal to the number of bins minus six, the number of parameters for the fifth-order polynomial [55].

In Section III E we estimate bounds on ϵ for various Z' masses based on the CMS results of Ref. [11], and in Section III F we estimate the potential sensitivity of 7 TeV LHC data using two hypothetical analyses with 1-GeV $m_{\mu\mu}$ bins, one with the $(p_T)_{\mu\mu} > 23$ GeV cut and the other without. Tables II–IV show the $M_{Z'}$ values tested for each analysis and the associated $m_{\mu\mu}$ ranges. For each $m_{\mu\mu}$ range, the third column of the table gives the median p -value for the fifth-order polynomial fit to pseudo data generated by statistically fluctuating Monte Carlo expectations for SM bin counts. We use the Monte Carlo expectations reported by CMS for the analysis based on the CMS results, and we use our own Monte Carlo simulations for the 1-GeV analyses

We choose κ values by imposing two requirements. First, we require that the median p value for background-model fits to SM Monte-Carlo-generated psuedo data is at least 0.5. Second, we require that when a signal corresponding to kinetic mixing parameter ϵ_{in} is injected into these pseudo-data sets, the 95% confidence level upper bound on ϵ , ϵ_{95} , is found to be less than ϵ_{in} for fewer than 5% of the pseudo-data sets. Our procedure for calculating ϵ_{95} for a particular data set is described in the following section. Because we impose the second requirement independently for each hypothesized value of $M_{Z'}$, different values of $M_{Z'}$ can have different values of κ . For each value of $M_{Z'}$, the second requirement is imposed over a range of ϵ_{in} values extending down to zero and up to twice the median of the ϵ_{95} values obtained for the SM-only pseudo-data sets. The κ values obtained by imposing

our two requirements fill the fourth column in Tables II–IV.

The κ parameter is meant to take into account imperfections in the polynomial background model. An actual experimental analysis would deal with systematic effects not considered here, and these effects may make the background $m_{\mu\mu}$ distribution less smooth than our Monte Carlo simulations would suggest. Along with the κ values given in Tables II–IV, we present results for $\kappa = 0$, $\kappa = 10^{-2}$, $\kappa = 2 \times 10^{-2}$, and $\kappa = 3 \times 10^{-2}$ to give a sense of how the potential sensitivity is affected if systematic effects introduce an additional source of bin-to-bin randomness.

D. Statistical procedure

Given a hypothesized value of $M_{Z'}$ and an observed invariant mass distribution n_i – which could either stand for actual data reported by CMS in Ref. [11], or for pseudo data generated from our Monte Carlo simulations – we use the CL_s method [48] to determine ϵ_{95} , the 95% confidence level upper limit on the kinetic mixing parameter for that value of $M_{Z'}$. We use a test statistic based on the χ^2 defined in Equation (12):

$$q_\mu = \begin{cases} \chi^2(\mu) - \chi^2(\hat{\mu}) & \mu > \hat{\mu} \\ 0 & \mu \leq \hat{\mu}, \end{cases} \quad (14)$$

where $\hat{\mu}$, is the best-fit signal strength. Using the asymptotic formulae of Ref. [49], we can approximate CL_s as

$$CL_s = \frac{1 - \Phi(\sqrt{q_\mu})}{1 - \Phi(\sqrt{q_{\mu,A}})}, \quad (15)$$

where Φ is the cumulative distribution of the standard Gaussian and $q_{\mu,A}$ is the value of q_μ obtained when the data n_i are taken to be equal to $\nu_i(0, \theta_{(0)}, \delta_{(0)})$, the expected bin counts for the best-fit background model. For the purpose of calculating $q_{\mu,A}$, we replace δ_i is with $\delta_i - \delta_{(0)i}$ in the χ^2 expression of Equation (12). We define ϵ_{95} to be the kinetic mixing parameter that gives $CL_s = 0.05$ for $\mu = 1$.

E. Estimates of bounds on ϵ from the 7 TeV CMS analysis

Focusing on the 30 – 76 GeV bins, the smoothness of the $m_{\mu\mu}$ distribution for the data shown in Figure 1 of the CMS analysis of Ref. [11] implies a constraint on the couplings

of a Z' with a mass in this range. We use the background model and statistical procedure outlined in Sections III C and III D to estimate upper bounds on ϵ based on the CMS results. The Z' masses tested, associated $m_{\mu\mu}$ fit ranges, and κ values are shown in Table II.

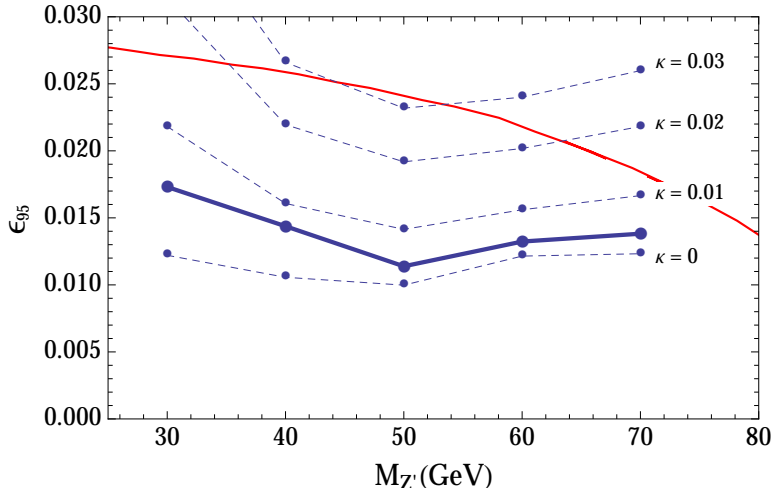


FIG. 5. Estimated 95% CL upper bounds on ϵ based on Ref. [11], the $\sqrt{s} = 7$ TeV CMS study of the dimuon invariant mass distribution. For the thick blue line, κ is set according to the procedure described in Section III C. The dashed lines show results for other κ values. The thin red line is the precision electroweak constraint taken from Ref. [25].

Based on the reported data bin counts from Figure 1 of Ref. [11], we obtain the ϵ_{95} estimates presented in Figure 5. The estimated ϵ bounds corresponding to the κ values of Table II lie below precision electroweak constraints by as much as a factor of two. Of the five masses tested, the four lowest lie on the boundary between two of the invariant mass bins used in the CMS analysis, meaning that the signal events are roughly equally distributed between two relatively wide mass bins. This pushes our estimates in the conservative direction, as far as other masses are concerned.

F. Sensitivity estimates for 7 TeV data

A more specialized analysis of LHC data could probe lower values of ϵ and a broader range of Z' masses. To estimate the potential sensitivity of $\sqrt{s} = 7$ TeV data we calculate median values of ϵ_{95} for fake data generated from our Drell-Yan Monte Carlo simulations. Although it would be more interesting for the LHC to find evidence for a light Z' rather

than to rule out additional parameter space, we use potential exclusion sensitivity in the absence of new physics as a diagnostic for whether new parameter space can be probed.

We consider two hypothetical analyses with 1 GeV $m_{\mu\mu}$ bins, both based on the same integrated luminosity as the CMS analysis. For the first, which incorporates the same muon p_T and η cuts as the CMS analysis, we use the Z' masses, $m_{\mu\mu}$ fit ranges, and κ values from Table III. The second analysis adds the cut $(p_T)_{\mu\mu} > 23$ GeV, and has been tested with the Z' masses, $m_{\mu\mu}$ fit ranges, and κ values from Table IV. We normalize our Monte Carlo simulations so that, in the absence of the $(p_T)_{\mu\mu}$ cut, we get the same number of selected events in the $60 - 120$ $m_{\mu\mu}$ range as the CMS analysis, as determined using Figure 1 of Ref. [11].

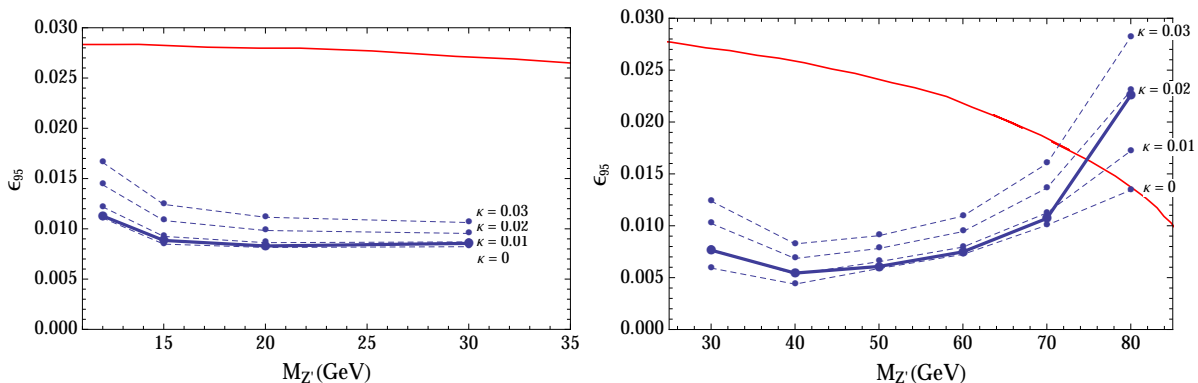


FIG. 6. Exclusion sensitivity estimates for 7 TeV LHC data based on an integrated luminosity of 4.5 fb^{-1} , with the cut $(p_T)_{\mu\mu} > 23$ GeV (left), and without a $(p_T)_{\mu\mu}$ cut (right). For the thick blue line, κ is set according to the procedure described in Section III C. The dashed lines show results for other κ values. The thin red line is the precision electroweak constraint taken from Ref. [25].

Our resulting sensitivity estimates are shown in Figure 6. For the κ values of Tables III and IV, the median values of ϵ_{95} go as low as a factor of four below the upper bound on ϵ from precision electroweak constraints.

IV. POTENTIAL SENSITIVITY OF 8 TEV AND 14 TEV LHC DATA

At $\sqrt{s} = 8$ TeV, the advantages of a larger integrated luminosity $\sim 20 \text{ fb}^{-1}$ and slightly higher signal cross sections compete against higher muon p_T thresholds required by the higher instantaneous luminosity. Based on Ref. [50], we conclude that it is realistic to

consider hypothetical analyses based on muon p_T cuts of 20 GeV and 10 GeV. These cuts push the peak in the $m_{\mu\mu}$ invariant mass distribution to larger values of $m_{\mu\mu}$, as shown in Figure 7.

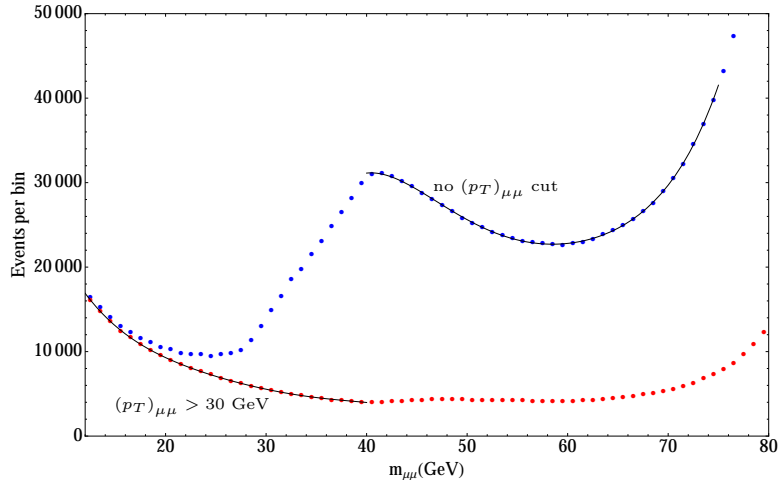


FIG. 7. For $\sqrt{s} = 8$ TeV and an integrated luminosity of 20 fb^{-1} , our simulated Drell-Yan $m_{\mu\mu}$ distributions with and without the $(p_T)_{\mu\mu}$ cut, along with best-fit fifth-order polynomial curves. The muons are required to have $(p_T)_1 > 20$ GeV, $(p_T)_2 > 10$ GeV, and $|\eta| < 2.4$.

As for the 7 TeV case, we consider two hypothetical analyses with 1-GeV $m_{\mu\mu}$ bins, one with a $(p_T)_{\mu\mu}$ cut and one without. We take the integrated luminosity to be 20 fb^{-1} . Fifth-order polynomial fits to our Drell-Yan Monte Carlo $m_{\mu\mu}$ distributions for the 12 – 40 and 40 – 75 GeV mass ranges are shown in Figure 7. Tables V and VI show the Z' masses tested for these analyses, the associated $m_{\mu\mu}$ ranges, and the κ values determined the procedure described in Section III C.

As before we apply a 75% efficiency for the signal. We normalize our Drell-Yan Monte Carlo simulations by requiring that the number of events in the 60 – 120 GeV $m_{\mu\mu}$ mass range is equal to the number of events in that mass range for the 7 TeV case, multiplied by by three factors: the ratio of the 8 and 7 TeV integrated luminosities, the ratio of the 8 and 7 TeV acceptances in that $m_{\mu\mu}$ range for the relevant muon p_T and η cuts, as determined by our simulations, and the ratio of the 8 and 7 TeV NNLO dimuon production cross sections in that $m_{\mu\mu}$ range. We use $\sigma_{8 \text{ TeV}} = 1.12 \text{ nb}$ and $\sigma_{7 \text{ TeV}} = 0.97 \text{ nb}$, consistent with the values shown in Refs. [51] based on calculations using FEWZ [52].

Our sensitivity estimates are shown in Figure 8. These results suggest that, relative to

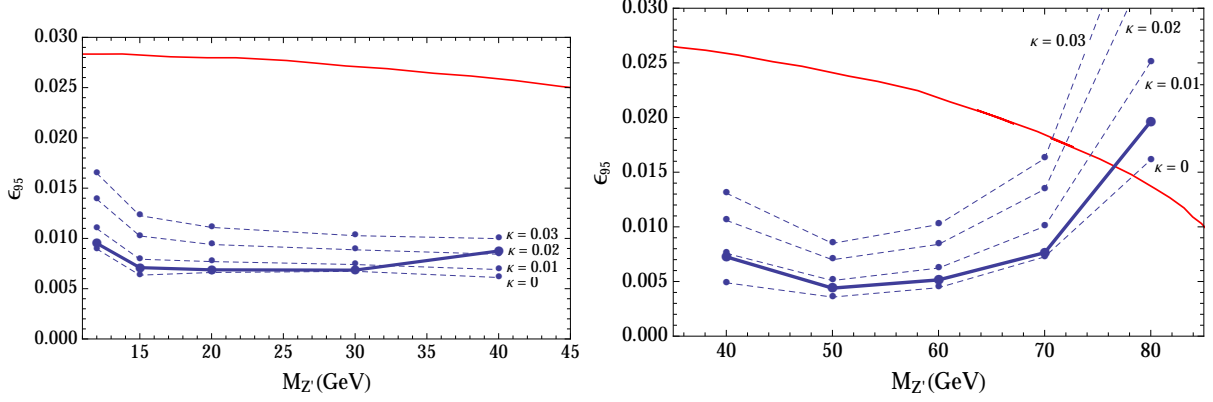


FIG. 8. Exclusion sensitivity estimates for 8 TeV LHC data based on an integrated luminosity of 20 fb^{-1} , with the cut $(p_T)_{\mu\mu} > 30 \text{ GeV}$ (left), and without a $(p_T)_{\mu\mu}$ cut (right). For the thick blue line, κ is set according to the procedure described in Section III C. The dashed lines show results for other κ values. The thin red line is the precision electroweak constraint taken from Ref. [25].

the 7 TeV case, an analysis based on 8 TeV data would yield improved sensitivity for at least some of the $m_{\mu\mu}$ range below the Z mass. Figure 9 collects our results for estimated bounds on ϵ based on the 7 TeV CMS analysis along with estimates of potential sensitivity for 7 and 8 TeV.

The ability of the 14 TeV LHC to probe relatively light dilepton resonances depends on trigger issues. Refs. [53, 54] give reason to hope that various upgrades should allow trigger thresholds to be close to their 8 TeV values, even at the High Luminosity LHC. We will estimate the 14 TeV reach for the kinetically mixed Z' model under the assumption that the dimuon p_T cuts we considered for 8 TeV analyses would be feasible at 14 TeV.

For the mass range considered here, our simulations indicate that the ϵ reach for 14 TeV and an integrated luminosity of 10 fb^{-1} is approximately the same as the reach for 8 TeV and an integrated luminosity of 20 fb^{-1} . If we optimistically assume that the sensitivity for higher luminosities depends on S/\sqrt{B} , and therefore that the ϵ reach is proportional to $(\int \mathcal{L} dt)^{-1/4}$, we obtain the 14 TeV sensitivity estimates shown in Figure 9 for an integrated luminosity of 3000 fb^{-1} . These reach down to $\epsilon \sim 10^{-3}$.

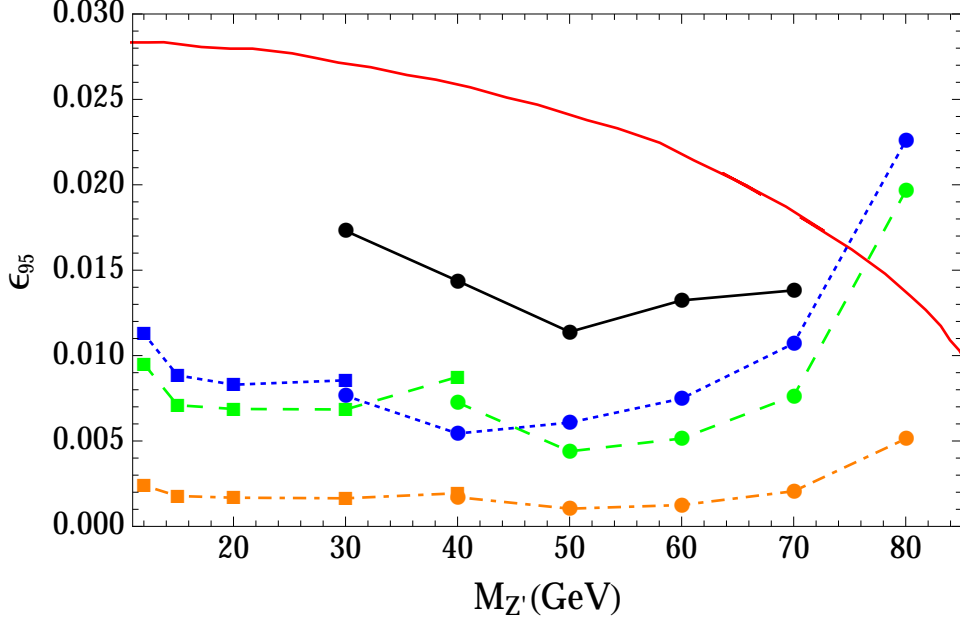


FIG. 9. Estimated upper bounds on ϵ based on the CMS analysis of Ref. [11] (black, solid), and exclusion sensitivity estimates for 7 TeV LHC data (blue, short dashed), for 8 TeV LHC data (green, long dashed), and, under the assumptions stated in the text, for 3000 fb $^{-1}$ of 14 TeV data (orange, dot-dashed). Results for the low-mass analyses incorporating a $(p_T)_{\mu\mu}$ cut are indicated by square markers. The κ parameters are set according to the procedure described in Section III C. The thin red line is the precision electroweak constraint taken from Ref. [25].

V. CONCLUSIONS

LHC measurements of dilepton invariant mass distributions below M_Z can be used as sensitive probe of new physics. For the kinetically mixed Z' model, analyses of 7 and 8 TeV data would be sensitive to ϵ values several times smaller than the upper bounds from precision electroweak constraints. If trigger thresholds can be held near their 8 TeV values, ϵ values as small as $\sim 10^{-3}$ may be accessible to the High Luminosity LHC.

ACKNOWLEDGMENTS

We are grateful to Kyle Cranmer, David Curtin, Stefania Gori, and Abi Sofer for helpful conversations. This work was supported by NSF Grant #1216168. DTS thanks the Aspen Center for Physics and NSF Grant #1066293 for hospitality as this paper was being

completed.

-
- [1] B. Holdom, Phys. Lett. B **166**, 196 (1986).
 - [2] C. Boehm and P. Fayet, Nucl. Phys. B **683**, 219 (2004) [hep-ph/0305261].
 - [3] M. Pospelov, A. Ritz and M. B. Voloshin, Phys. Lett. B **662**, 53 (2008) [arXiv:0711.4866 [hep-ph]].
 - [4] R. Foot, Phys. Rev. D **78**, 043529 (2008) [arXiv:0804.4518 [hep-ph]].
 - [5] N. Arkani-Hamed, D. P. Finkbeiner, T. R. Slatyer and N. Weiner, Phys. Rev. D **79**, 015014 (2009) [arXiv:0810.0713 [hep-ph]].
 - [6] H. An, S. -L. Chen, R. N. Mohapatra and Y. Zhang, JHEP **1003**, 124 (2010) [arXiv:0911.4463 [hep-ph]].
 - [7] E. J. Chun, J. -C. Park and S. Scopel, JHEP **1102**, 100 (2011) [arXiv:1011.3300 [hep-ph]].
 - [8] S. Andreas, M. D. Goodsell and A. Ringwald, Phys. Rev. D **87**, 025007 (2013) [arXiv:1109.2869 [hep-ph]].
 - [9] H. Davoudiasl and I. M. Lewis, Phys. Rev. D **89**, 055026 (2014) [arXiv:1309.6640 [hep-ph]].
 - [10] J. M. Cline, G. Dupuis, Z. Liu and W. Xue, arXiv:1405.7691 [hep-ph].
 - [11] S. Chatrchyan *et al.* [CMS Collaboration], JHEP **1312**, 030 (2013) [arXiv:1310.7291 [hep-ex]].
 - [12] S. Chatrchyan *et al.* [CMS Collaboration], Phys. Rev. Lett. **109**, 121801 (2012) [arXiv:1206.6326 [hep-ex]].
 - [13] K. S. Babu, C. F. Kolda and J. March-Russell, Phys. Rev. D **57**, 6788 (1998) [hep-ph/9710441].
 - [14] T. G. Rizzo, Phys. Rev. D **59**, 015020 (1998) [hep-ph/9806397].
 - [15] M. J. Strassler and K. M. Zurek, Phys. Lett. B **651**, 374 (2007) [hep-ph/0604261].
 - [16] J. Kumar and J. D. Wells, Phys. Rev. D **74**, 115017 (2006) [hep-ph/0606183].
 - [17] W. -F. Chang, J. N. Ng and J. M. S. Wu, Phys. Rev. D **74**, 095005 (2006) [Erratum-ibid. D **79**, 039902 (2009)] [hep-ph/0608068].
 - [18] D. Feldman, Z. Liu and P. Nath, Phys. Rev. D **75**, 115001 (2007) [hep-ph/0702123 [HEP-PH]].
 - [19] N. Arkani-Hamed and N. Weiner, JHEP **0812** (2008) 104 [arXiv:0810.0714 [hep-ph]].
 - [20] S. Cassel, D. M. Ghilencea and G. G. Ross, Nucl. Phys. B **827**, 256 (2010) [arXiv:0903.1118 [hep-ph]].

- [21] B. Batell, M. Pospelov and A. Ritz, Phys. Rev. D **79**, 115008 (2009) [arXiv:0903.0363 [hep-ph]].
- [22] R. Essig, P. Schuster and N. Toro, Phys. Rev. D **80**, 015003 (2009) [arXiv:0903.3941 [hep-ph]].
- [23] J. D. Bjorken, R. Essig, P. Schuster and N. Toro, Phys. Rev. D **80**, 075018 (2009) [arXiv:0906.0580 [hep-ph]].
- [24] B. Batell, M. Pospelov and A. Ritz, Phys. Rev. D **80**, 095024 (2009) [arXiv:0906.5614 [hep-ph]].
- [25] A. Hook, E. Izaguirre and J. G. Wacker, Adv. High Energy Phys. **2011**, 859762 (2011) [arXiv:1006.0973 [hep-ph]].
- [26] M. Williams, C. P. Burgess, A. Maharana and F. Quevedo, JHEP **1108**, 106 (2011) [arXiv:1103.4556 [hep-ph]].
- [27] M. T. Frandsen, F. Kahlhoefer, A. Preston, S. Sarkar and K. Schmidt-Hoberg, JHEP **1207**, 123 (2012) [arXiv:1204.3839 [hep-ph]].
- [28] N. Toro and I. Yavin, Phys. Rev. D **86**, 055005 (2012) [arXiv:1202.6377 [hep-ph]].
- [29] V. Barger, D. Marfatia and A. Peterson, Phys. Rev. D **87**, 015026 (2013) [arXiv:1206.6649 [hep-ph]].
- [30] J. Jaeckel, M. Jankowiak and M. Spannowsky, Phys. Dark Univ. **2**, 111 (2013) [arXiv:1212.3620 [hep-ph]].
- [31] H. Davoudiasl, H. -S. Lee, I. Lewis and W. J. Marciano, Phys. Rev. D **88**, no. 1, 015022 (2013) [arXiv:1304.4935 [hep-ph]].
- [32] D. Hooper, N. Weiner and W. Xue, Phys. Rev. D **86**, 056009 (2012) [arXiv:1206.2929 [hep-ph]].
- [33] D. S. Akerib *et al.* [LUX Collaboration], Phys. Rev. Lett. **112**, 091303 (2014) [arXiv:1310.8214 [astro-ph.CO]].
- [34] J. Jaeckel, Frascati Phys. Ser. **56**, 172 (2012) [arXiv:1303.1821 [hep-ph]].
- [35] [ATLAS Collaboration], ATLAS-CONF-2013-017.
- [36] [CMS Collaboration], CMS PAS EXO-12-061.
- [37] J. Alwall, M. Herquet, F. Maltoni, O. Mattelaer and T. Stelzer, JHEP **1106**, 128 (2011) [arXiv:1106.0522 [hep-ph]].
- [38] S. Kretzer, H. L. Lai, F. I. Olness and W. K. Tung, Phys. Rev. D **69**, 114005 (2004) [hep-ph/0307022].

- [39] P. M. Nadolsky, H. -L. Lai, Q. -H. Cao, J. Huston, J. Pumplin, D. Stump, W. -K. Tung and C. -P. Yuan, Phys. Rev. D **78**, 013004 (2008) [arXiv:0802.0007 [hep-ph]].
- [40] R. Hamberg, W. L. van Neerven and T. Matsuura, Nucl. Phys. B **359**, 343 (1991) [Erratum-ibid. B **644**, 403 (2002)].
- [41] W. L. van Neerven and E. B. Zijlstra, Nucl. Phys. B **382**, 11 (1992) [Erratum-ibid. B **680**, 513 (2004)].
- [42] [ATLAS Collaboration], ATLAS-CONF-2011-020.
- [43] N. D. Christensen and C. Duhr, Comput. Phys. Commun. **180**, 1614 (2009) [arXiv:0806.4194 [hep-ph]].
- [44] T. Sjostrand, S. Mrenna and P. Z. Skands, JHEP **0605**, 026 (2006) [hep-ph/0603175].
- [45] J. Alwall, S. Hoche, F. Krauss, N. Lavesson, L. Lonnblad, F. Maltoni, M. L. Mangano and M. Moretti *et al.*, Eur. Phys. J. C **53**, 473 (2008) [arXiv:0706.2569 [hep-ph]].
- [46] J. de Favereau *et al.* [DELPHES 3 Collaboration], JHEP **1402**, 057 (2014) [arXiv:1307.6346 [hep-ex]].
- [47] G. Aad *et al.* [ATLAS Collaboration], JHEP **1406**, 112 (2014) [arXiv:1404.1212 [hep-ex]].
- [48] A. L. Read, J. Phys. G **28**, 2693 (2002).
- [49] G. Cowan, K. Cranmer, E. Gross and O. Vitells, Eur. Phys. J. C **71**, 1554 (2011) [arXiv:1007.1727 [physics.data-an]].
- [50] S. Chatrchyan *et al.* [CMS Collaboration], JHEP **1401**, 096 (2014) [arXiv:1312.1129 [hep-ex]].
- [51] S. Chatrchyan *et al.* [CMS Collaboration], Phys. Rev. Lett. **112**, 191802 (2014) [arXiv:1402.0923 [hep-ex]].
- [52] R. Gavin, Y. Li, F. Petriello and S. Quackenbush, Comput. Phys. Commun. **182**, 2388 (2011) [arXiv:1011.3540 [hep-ph]].
- [53] [ATLAS Collaboration], ATL-PHYS-PUB-2013-004.
- [54] A. Tapper *et al.* [CMS Collaboration], CERN-LHCC-2013-011.
- [55] Starting with pseudo data sets generated by statistically fluctuating the background-model prediction $b_i(\theta_{(0)}, \delta_{(0)})$, and associated sets of δ_i^{fake} generated by fluctuating about $\delta_{(0)i}$ with standard deviation κ , the p -value that we have defined is the fraction of those pseudo data/ δ_i^{fake} sets for which $\chi^2(0)$ is greater than for the original data set. When calculating $\chi^2(0)$ for the pseudo data sets, one replaces δ_i with $\delta_i - \delta_i^{\text{fake}}$ in Equation (12).

$M_{Z'}$ (GeV)	$\sigma_{7 \text{ TeV}}$ (pb)	$\sigma_{8 \text{ TeV}}$ (pb)	$\sigma_{14 \text{ TeV}}$ (pb)
12	274	305	476
15	163	182	288
20	80.6	90.3	147
30	28.5	32.4	54.6
40	13.3	15.3	26.3
50	7.43	8.56	15.1
60	4.76	5.51	9.96
70	3.60	4.21	7.70
80	4.24	4.94	9.28

TABLE I. Cross sections for $pp \rightarrow Z' \rightarrow \mu^+ \mu^-$ used for our analyses, taking $\epsilon = 2 \times 10^{-2}$. The cross sections are proportional to ϵ^2 .

$M_{Z'}$ (GeV)	$m_{\mu\mu}$ range (GeV)	median p -value, $\kappa \rightarrow 0$	κ
30	30 – 76	0.20	6.1×10^{-3}
40	35 – 76	0.25	7.5×10^{-3}
50	35 – 76	0.25	4.8×10^{-3}
60	35 – 76	0.25	4.8×10^{-3}
70	35 – 76	0.25	4.8×10^{-3}

TABLE II. Masses tested for the analysis based on the CMS results of Ref. [11], and associated fit information. The third column gives the median p -value for the polynomial ($\kappa \rightarrow 0$) fit to pseudo data sets generated by statistically fluctuating the CMS Monte-Carlo-predicted SM bin counts reported in Figure 1 of Ref. [11]. No $(p_T)_{\mu\mu}$ cut is imposed in this analysis.

$M_{Z'}$ (GeV)	$m_{\mu\mu}$ range (GeV)	median p -value, $\kappa \rightarrow 0$	κ
30	30 – 60	0.26	9.6×10^{-3}
40	35 – 75	0.27	1.1×10^{-2}
50	35 – 75	0.27	4.9×10^{-3}
60	35 – 75	0.27	4.9×10^{-3}
70	35 – 75	0.27	7.2×10^{-3}
80	60 – 82	0.21	1.9×10^{-2}

TABLE III. Masses tested for the $\sqrt{s} = 7$ TeV analysis based on 1-GeV bins and no $(p_T)_{\mu\mu}$ cut, and associated fit information. The third column gives the median p -value for the polynomial ($\kappa \rightarrow 0$) fit to pseudo data sets generated by statistically fluctuating our simulated Drell-Yan $m_{\mu\mu}$ distribution.

$M_{Z'}$ (GeV)	$m_{\mu\mu}$ range (GeV)	median p -value, $\kappa \rightarrow 0$	κ
12	12 – 40	0.38	6.0×10^{-3}
15	12 – 40	0.38	6.0×10^{-3}
20	12 – 40	0.38	6.0×10^{-3}
30	12 – 40	0.38	9.2×10^{-3}

TABLE IV. Masses tested for the $\sqrt{s} = 7$ TeV analysis based on 1-GeV bins with a $(p_T)_{\mu\mu} > 23$ GeV cut, and associated fit information. The third column gives the median p -value for the polynomial ($\kappa \rightarrow 0$) fit to pseudo data sets generated by statistically fluctuating our simulated Drell-Yan $m_{\mu\mu}$ distribution.

$M_{Z'}$ (GeV)	$m_{\mu\mu}$ range (GeV)	median p -value, $\kappa \rightarrow 0$	κ
40	40 – 75	0.28	9.1×10^{-3}
50	40 – 75	0.28	6.6×10^{-3}
60	40 – 75	0.28	5.3×10^{-3}
70	40 – 75	0.28	2.6×10^{-3}
80	65 – 82	0.38	5.0×10^{-3}

TABLE V. Masses tested for the $\sqrt{s} = 8$ TeV analysis with no $(p_T)_{\mu\mu}$ cut, and associated fit information. The third column gives the median p -value for the polynomial ($\kappa \rightarrow 0$) fit to pseudo data sets generated by statistically fluctuating our simulated Drell-Yan $m_{\mu\mu}$ distribution.

$M_{Z'}$ (GeV)	$m_{\mu\mu}$ range (GeV)	median p -value, $\kappa \rightarrow 0$	κ
12	12 – 40	0.32	4.5×10^{-3}
15	12 – 40	0.32	6.2×10^{-3}
20	12 – 40	0.32	4.5×10^{-3}
30	12 – 40	0.32	4.5×10^{-3}
40	12 – 45	0.21	2.2×10^{-2}

TABLE VI. Masses tested for the $\sqrt{s} = 8$ TeV analysis with a $(p_T)_{\mu\mu} > 30$ GeV cut, and associated fit information. The third column gives the median p -value for the polynomial ($\kappa \rightarrow 0$) fit to pseudo data sets generated by statistically fluctuating our simulated Drell-Yan $m_{\mu\mu}$ distribution.